THE JOURNAL OF BIOLOGICAL CHEMISTRY VOL. 285, NO. 27, pp. 20625–20633, July 2, 2010


# $GABA_B$ Receptor Constituents Revealed by Tandem Affinity Purification from Transgenic Mice*

Received for publication, July 28, 2009, and in revised form, April 17, 2010 Published, JBC Papers in Press, April 20, 2010, DOI 10.1074/jbc.M109.049700

**Tudor Bartoi[‡], Kristoffer T. G. Rigbolt[§], Dan Du[¶], Georg Köhr[¶], Blagoy Blagoev[§], and Hans-Christian Kornau[‡1]**

*From the [‡]Center for Molecular Neurobiology (ZMNH), University of Hamburg, Falkenried 94, D-20251 Hamburg, Germany, the [§]Center for Experimental BioInformatics (CEBI), Department of Biochemistry and Molecular Biology, University of Southern Denmark, Campusvej 55, DK-5230 Odense M, Denmark, and the [¶]Department of Molecular Neurobiology, Max Planck Institute for Medical Research, Jahnstrasse 29, D-69120 Heidelberg, Germany*

**$GABA_B$ receptors function as heterodimeric G-protein-coupled receptors for the neurotransmitter γ-aminobutyric acid (GABA). Receptor subtypes, based on isoforms of the ligand-binding subunit $GABA_{B1}$, are thought to involve a differential set of associated proteins. Here, we describe two mouse lines that allow a straightforward biochemical isolation of $GABA_B$ receptors. The transgenic mice express $GABA_{B1}$ isoforms that contain sequences for a two-step affinity purification, in addition to their endogenous subunit repertoire. Comparative analyses of purified samples from the transgenic mice and wild-type control animals revealed two novel components of the $GABA_{B1}$ complex. One of the identified proteins, potassium channel tetramerization domain-containing protein 12, associates with heterodimeric $GABA_B$ receptors via the $GABA_{B2}$ subunit. In transfected hippocampal neurons, potassium channel tetramerization domain-containing protein 12 augmented axonal surface targeting of $GABA_{B2}$. The mice equipped with tags on $GABA_{B1}$ facilitate validation and identification of native binding partners of $GABA_B$ receptors, providing insight into the molecular mechanisms of synaptic modulation.**

$GABA_B$ receptors convey the metabotropic action of GABA,[2] the main inhibitory neurotransmitter in the brain (1). They are concentrated at axonal boutons of GABAergic and glutamatergic neurons as well as in dendritic spines and shafts at extrasynaptic sites (2). Presynaptic $GABA_B$ receptors primarily inhibit calcium channels regulating evoked neurotransmitter release, whereas postsynaptic $GABA_B$ receptors mainly open G-protein-regulated inwardly rectifying potassium channels and thereby elicit slow inhibitory postsynaptic potentials. Additionally, $GABA_B$ receptor activation decreases the local cAMP level. $GABA_B$ receptors function as heteromeric G-protein-coupled receptors consisting of two subunits, $GABA_{B1}$ and $GABA_{B2}$. Heterodimerization is a prerequisite for both surface trafficking of the receptor and ligand-stimulated activation of a $G_{i/o}$-protein (3).

Two N-terminal $GABA_{B1}$ variants, termed $GABA_{B1a}$ and $GABA_{B1b}$ differing only by a pair of sushi repeats that is exclusively present in $GABA_{B1a}$, have been identified (4). They originate from the use of alternative transcriptional start sites (3, 5, 6) and underlie functional subtypes of the $GABA_B$ receptor with differential localization to pre- and postsynaptic sites in hippocampus and cortex (7–9). Because the sushi repeats are the only difference between $GABA_{B1a}$ and $GABA_{B1b}$, it is to be expected that proteins interacting with these domains target or retain the $GABA_{B1a}$ isoform to specific microdomains. Consistently, a soluble recombinant protein of the two sushi repeats binds to neuronal membranes with low nanomolar affinity (10). An interaction of one of the two sushi repeats with fibulin-2 has been described (11), but the functional implication remains elusive.

Further subtypes of the $GABA_B$ receptor may be formed by a compartment-specific interaction of additional proteins, *e.g.* effector channels, with the core $GABA_B$ receptor complex (12). Furthermore, $GABA_{B1}$ can associate with seven-transmembrane proteins differently from $GABA_{B2}$ and may thereby modulate the signal transduction of other receptor systems (13, 14). Using the intracellular C-terminal domains of the $GABA_B$ receptor subunits as bait in genetic screens for interactors like the yeast two-hybrid system, a number of proteins ranging from transcription factors and RNA-binding proteins over trafficking factors to cytoskeletal elements and scaffolding proteins were identified (3, 15, 16). However, the native interactions of the $GABA_B$ receptor as an integral membrane protein complex may only be readily uncovered by biochemical isolation of the protein complex from brain membrane preparations followed by mass spectrometry analysis. The direct approach, immunoprecipitation of solubilized $GABA_B$ receptor complexes, relies on antisera that recognize the native conformation of $GABA_{B1}$ or $GABA_{B2}$ with high efficiency and specificity. As an alternative, tandem affinity purification (TAP) may be applied with the advantage of two consecutive purification steps under native conditions (17). In *Saccharomyces cerevisiae* the TAP strategy allowed the generation of a large protein interaction map (18). TAP proved useful in mammalian approaches as well (19–21). The first TAP-based transgenic mouse proteomics approach

* This work was supported in part by the Deutsche Forschungsgemeinschaft (SFB444).

[1] To whom correspondence should be addressed. Tel.: 49-40-7410-58228; Fax: 49-40-7410-58364; E-mail: hckornau@zmnh.uni-hamburg.de.

[2] The abbreviations used are: GABA, γ-aminobutyric acid; AMPA, α-amino-3-hydroxy-5-methyl-4-isoxazole propionic acid; BAC, bacterial artificial chromosome; CBP, calmodulin-binding peptide; EPSC, excitatory postsynaptic current; GRP78, glucose-regulated protein 78; HA, hemagglutinin; IPSC, inhibitory postsynaptic current; KCTD12, potassium channel tetramerization domain-containing protein 12; MAP2, microtubule-associated protein 2; P*n*, postnatal day *n*; ProtA, protein A; SBP, streptavidin-binding peptide; T1 domain, voltage-gated potassium channel tetramerization domain; TAP, tandem affinity purification; TEV, tobacco etch virus; EGFP, enhanced green fluorescent protein; PBS, phosphate-buffered saline; BSA, bovine serum albumin.

targeted interactions of 14-3-3 proteins, very abundant cytoplasmic regulators of cell signaling, and revealed almost 40 novel 14-3-3ζ-binding proteins (22). A TAP search for proteins binding to melatonin receptors stably expressed in HEK293 cells showed that this approach is also suitable to isolate G-protein-coupled receptor complexes from a cellular environment (23).

Here, we describe TAP of $GABA_B$ receptor complexes from mouse brain including genetic engineering of mice and analyses of purified fractions by immunoblotting and high accuracy mass spectrometry. The identification of two novel components of native $GABA_B$ receptors validated the approach.

## EXPERIMENTAL PROCEDURES

*DNA Constructs*—Constructs for heterologous expression of rat $GABA_{B1a}$ (GenBank™ accession number Y10369), HA-$GABA_{B1a}$, HA-SBP-$GABA_{B1a}$, rat $GABA_{B2}$ (GenBank™ accession number AF109405), HA-$GABA_{B2}$, HA-$GABA_{B2}$Δ921–940, and HA-$GABA_{B2}$Δ817–940, were generated using a cytomegalovirus expression vector (24). Constructs for the expression of $GABA_{B1a}$-CBP-TEV-ProtA, rat $GABA_{B1b}$(Y10370)-CBP-TEV-ProtA, mouse KCTD12 (GenBank™ accession number NM_177715), and HA-$GABA_{B2}$(817–920) were generated in pcDNA3. The N-terminal tags HA (amino acid sequence YPYDVPDYA) and HA-SBP (25) directly follow the signal sequence or the start methionine, the C-terminal tags, CBP-TEV-ProtA (17), and HA, the last amino acids of the wild-type proteins. pEGFP-C2 was used for the generation of fusion proteins of EGFP with KCTD12, KCTD12-T1 (amino acids 1–134), and KCTD12-CT (amino acids 135–327).

*Antibodies*—The purchased primary antibodies used for Western blotting were: CASK (610782, BD Biosciences, 1:1000), $GABA_{B1}$ (sc-14006, Santa Cruz Biotechnology; 1:1000; AB1531, Millipore, 1:2000), GFP (ab6556, Abcam, 1:5000), GRP78 (ab21685, Abcam, 1:200), NSF (612272, BD Biosciences, 1:5000), PSD-95 (MA1-046, ABR, 1:2000), and HA (HA.11, Covance, 1:1000). The antibody to $GABA_{B2}$ has been described previously (26). Polyclonal antibody to KCTD12 was raised in rabbits against a synthetic peptide corresponding to amino acid residues 254–267 in mouse KCTD12 coupled to *Limulus polyphemus* hemocyanin (Biogenes). The antiserum was affinity-purified using the immunogenic peptide.

*Cell Culture*—Growth media and additives were purchased from Invitrogen. The cell lines were grown following standard protocols. Primary hippocampal neurons were prepared from newborn rats (postnatal day (P) 0–P1) and plated on 12-mm glass coverslips coated with laminin and poly-L-lysine (Sigma-Aldrich) at a density of $10^5$ cells/well in 24-well plates.

*Bacterial Artificial Chromosome (BAC) Modification by ET Cloning*—BAC citb544e14 (AF532114), kindly provided by Kirsten Fischer Lindahl, was modified by homologous recombination in *Escherichia coli* HS996 following previously described protocols (27). A cassette consisting of the CBP-TEV-ProtA tag sequence and a kanamycin resistance gene was inserted into exon 18 of the $GABA_{B1}$ gene (6), directly 5′ to the stop codon (between nucleotides 146573 and 146574 of BAC citb544e14), using pBAD-ETγ (27). Independently, a cassette encompassing the counterselection genes *SacB* (28) and *RpsL* (29) and a kanamycin resistance gene was inserted into $GABA_{B1a}$ exon 1a2 (6), directly 3′ to the sequence encoding the signal peptide (between nucleotides 120,273 and 120,274 of BAC citb544e14) and replaced with an HA-SBP tag coding sequence using pGETrec (30), which was kindly provided by Panayiotis A. Ioannou. The integrity of recombinant clones was confirmed by Southern blotting and DNA sequencing.

*Generation of Transgenic Mouse Lines*—Transgenic mice were generated essentially as described (31). BACs were purified (Nucleobond AX500, Machery-Nagel), diluted at a concentration of approximately 0.5 μg/μl (10 mM Tris, pH 7.5, 0.5 mM EDTA, 30 nM spermine, 20 nM spermidine, 0.1 M NaCl), and microinjected into pronuclei resulting from F1-C57BL/6/CBA matings. The embryos were transferred to the oviduct of pseudopregnant F1-C57BL/6/CBA foster mothers. Progeny were genotyped by PCR analysis, and founders, in which the modified BAC randomly inserted into the genome, were mated onto a C57BL/6 background.

*Aequorin Assay*—Chinese hamster ovary/$G\alpha_{16}$/mtAEQ cells (32), kindly provided by Atanas Ignatov, permanently expressing both mitochondria-targeted apoaequorin and the G-protein α-subunit $G\alpha_{16}$, were plated into 96-well white/opaque microtiter plates (Nunc) and cotransfected with expression vectors for $GABA_{B2}$ and wild-type or modified $GABA_{B1a}$ using Lipofectamine (Invitrogen). Two days later, the cells were loaded with coelenterazine (Perkin-Elmer Life Sciences) for 4 h and stimulated with (*R*)-baclofen (Tocris) at concentrations ranging from 0.01 to 100 μM. The luminescent response was measured 15 s after stimulation using a microluminometer (MicroLumat Plus, Perkin-Elmer Life Sciences). The half-maximal effective concentration ($EC_{50}$) values for baclofen-stimulated G-protein coupling were calculated by fitting the relative light units into a sigmoidal dose-response curve using Origin 7.0 (Microcal software).

*In Situ Hybridization*—*In situ* hybridization on frozen mouse brain sections was performed as described previously (33). Briefly, the brains were frozen on solid $CO_2$, and 16-μm sections were prepared on a cryostat (CM 3050-S, Leica Microsystems) and collected onto microscope slides (SuperFrost Plus, Menzel). Sense and antisense [$^{35}$S]dUTP-labeled cRNA probes were generated by *in vitro* transcription (MAXIscript *in vitro* transcription kit, Ambion) of subcloned cDNA fragments. The probe sequences used were: B1a, nucleotides 1–488 of rat $GABA_{B1a}$ (Y10369); B1a/b pan, nucleotides 560–1062 of rat $GABA_{B1a}$; HA-SBP, sequence encoding HA-SBP; and CBP-TEV-ProtA, nucleotides 36–555 of the sequence for the TAP tag (17). The hybridized sections were exposed to Kodak Biomax MR film for 3–5 days, dipped in Kodak NTB-3 nuclear emulsion (both from GE Healthcare), exposed for 8 days to 3 weeks, and counterstained with Mayer's hemalaun.

*Electrophysiology*—Acute transverse hippocampal slices (250 μm) were prepared from young (P21–P31) transgenic and wild-type mice and recovered for 1 h (first at 31 °C for 30 min and then at room temperature for at least 30 min) before starting whole cell recordings at 31 °C. The slices were submerged and perfused at 2 ml/min with artificial cerebrospinal fluid (125 mM

NaCl, 25 mM $NaHCO_3$, 2.5 mM KCl, 1.25 mM $NaH_2PO4$, 1 mM $MgCl_2$, 2 mM $CaCl_2$, 25 mM glucose, pH 7.4, with 95% $O_2$, 5% $CO_2$). Excitatory or inhibitory postsynaptic currents (EPSCs or IPSCs) were electrically stimulated every 10 s by stimulating Schaffer collaterals in stratum radiatum ~150 μm from the pyramidal layer with a glass pipette filled with artificial cerebrospinal fluid. Patch pipettes had resistances of 4–6 megohm when filled with internal solution (130 mM cesium gluconate, 5.5 mM KCl, 10 mM HEPES, 1 mM EGTA, 4 mM MgATP, 0.5 mM $Na_3GTP$, 10 mM sodium phosphocreatine, 5 mM QX-314, pH 7.25, 280–290 mosmol). The liquid junction potential (16.3 mV) was corrected. EPSCs or IPSCs were recorded with an EPC9 (HEKA) at the reversal potential for GABA (−80 mV) or AMPA (0 mV), respectively. Baclofen (50 μM) and CGP54626 (5 μM) were kept as aliquots (stocks of 10 and 5 mM), and the solutions were freshly prepared on the day of the experiment. Holding currents were recorded in the presence of tetrodotoxin (1 μM) with patch electrodes containing 125 mM potassium gluconate, 10 mM sodium gluconate, 4 mM NaCl, 10 mM HEPES, 0.2 mM EGTA, 4 mM MgATP, 0.3 mM $Na_3GTP$, 10 mM sodium phosphocreatine (pH 7.25, 280–290 mosmol). The recordings were excluded if input resistance and/or series resistance changed by more than 20%. The values are the means ± S.E., and statistical significance between the three genotypes was tested using one-way analysis of variance.

*Extraction of Membrane Proteins from Mouse Brains*—All of the protein work was performed at 4 °C if not stated otherwise. Whole brains were homogenized (S. Potter, B. Braun Biotech) in sucrose buffer (320 mM sucrose, 1 mM $NaHCO_3$, 1 mM $MgCl_2$, 50 μM $CaCl_2$, protease inhibitors; Complete from Roche Applied Science), and the nuclei were removed (1,400 × *g* for 10 min). The membranes were pelleted (20,000 × *g* for 20 min), resuspended in solubilization buffer (400 mM NaCl, 10 mM Tris, pH 8.0, 1% Triton X-100, protease inhibitors), and incubated overnight on a rotator. The membrane debris was removed by ultracentrifugation (100,000 × *g* for 60 min). The resulting supernatant represents the solubilized membrane protein fraction.

*Tandem Affinity Purification from NTAP-$GABA_{B1a}$ Mice*—40–70 mg of solubilized membrane proteins were prepared from juvenile (P10–P16) mouse brains, and the 2-mercaptoethanol and EDTA concentrations were adjusted to 5 and 2 mM, respectively. The extract was rotated overnight with 720 μl of streptavidin-coated magnetic beads (Dynabeads MyOne Streptavidin T1, Invitrogen). Afterward, the beads were collected using a magnetic device (Invitrogen) and washed three times with 1 ml of solubilization buffer, and the bound material was eluted with 2 mM biotin in 1600 μl of solubilization buffer for 20 min on a rotating wheel. The biotin eluate was incubated with 160 μl of anti-HA affinity matrix (Roche Applied Science) rotating for 4 h. After the beads were washed three times with 1 ml of solubilization buffer, the bound material was eluted in SDS loading buffer (50 mM Tris-Cl, pH 8.0, 200 mM dithiothreitol, 6% (w/v) SDS, 10% glycerol, 7 M urea, 0.01% (w/v) bromphenol blue) for 10 min at 42 °C, separated on NuPage Novex gels (Invitrogen), and stained with silver nitrate as previously described (34).

*Tandem Affinity Purification from $GABA_{B1a/b}$-CTAP Mice*—The purification was basically performed as previously described (17). 40–70 mg of solubilized membrane proteins prepared from juvenile (P10–P16) mouse brains were incubated with 100 μl of IgG-Sepharose beads (GE Healthcare) rotating overnight. The beads were collected by centrifugation (1 min at 1,000 × *g*), washed three times with 1 ml of solubilization buffer, and resuspended in 300 μl of the same buffer. Bound material was eluted from the IgG matrix using 80 units of TEV protease (Invitrogen) shaking for 2 h at 16 °C. The supernatant was collected and mixed with 900 μl of calmodulin binding buffer (1% Triton X-100, 150 mM NaCl, 10 mM Tris-Cl, pH 7.5, 7.5 mM β-mercaptoethanol, 0.75 mM MgAc, 0.75 mM imidazole, 2 mM $CaCl_2$), and the $CaCl_2$ concentration of the suspension was adjusted to 2 mM. The suspension was incubated with 50 μl of calmodulin-agarose (Stratagene) rotating for 2 h. After washing the beads three times with 1 ml of calmodulin binding buffer, the bound material was eluted in SDS loading buffer and analyzed as described above.

*Mass Spectrometry Analysis*—The applied work flow followed an established protocol (35). Briefly, the protein bands were cut out of the gel and subjected to in-gel reduction of protein disulfide bonds using dithiothreitol and subsequent alkylation by the addition of iodoacetamide. Next, the protein content was digested with trypsin overnight at 37 °C, and the peptides were extracted from the gel and then concentrated and desalted by stop and go extraction (36, 37). The samples were analyzed by liquid chromatography-tandem mass spectrometry using an Agilent 1200 high performance liquid chromatography system connected online to an LTQ-Orbitrap XL (Thermo Fisher Scientific). Fragment spectra were recorded in the LTQ and high resolution and mass accuracy spectra on the intact peptides in the Orbitrap (38). Centroided peak lists were searched with Mascot v2.2 (Matrix Science) against the mouse international protein index (IPI) database (39).

*Coimmunoprecipitation*—Solubilized membrane proteins (6–18 mg) of juvenile wild-type C57BL/6 mouse brains were supplemented with 10 μg of monoclonal mouse anti-$GABA_{B1}$ antibody (ab55051, Abcam) or mouse IgG as a control (Sigma) and rotated overnight. The immune complexes were collected for 4 h on 50 μl of protein A beads (GE Healthcare), washed three times with 0.5 ml of solubilization buffer, and eluted in SDS loading buffer.

*Purification of HA-tagged Proteins from Transfected HEK293 Cells*—Two days after transfection with calcium phosphate, the cells were washed, harvested, resuspended in 600 μl of solubilization buffer, and rotated overnight. The extract was centrifuged for 1 h at 100,000 × *g*, and the supernatant was incubated with 20 μl of anti-HA affinity matrix (Roche Applied Science) rotating for 4 h. The matrix was washed three times with 0.5 ml of solubilization buffer, and the bound protein was eluted in SDS loading buffer.

*Immunofluorescence of Cultured Neurons*—Dissociated rat hippocampal neurons were transfected using calcium phosphate at day 7 *in vitro*. Two days later, the neurons were incubated with mouse anti-HA antibody (HA.11, Covance, 1:500) in the growth medium for 30 min at 10 °C. The neurons were washed with Dulbecco's modified Eagle's medium (Invitrogen),

fixed with 4% (w/v) paraformaldehyde, 4% (w/v) sucrose/PBS for 10 min, permeabilized with 0.25% Triton X-100/PBS for 10 min, and blocked with 1% (w/v) BSA/PBS for 30 min, and rabbit anti-mictrotubule-associated protein 2 (MAP2) antibody (Synaptic Systems, 1:1000) was applied in 1% (w/v) BSA/PBS for 1 h. The fixation and all subsequent steps were performed at room temperature. After three brief washes with 1% (w/v) BSA/PBS, species-specific secondary antibodies (donkey anti-mouse Alexa 546, Molecular Probes, 1:1000; donkey anti-rabbit Cy5, Jackson ImmunoResearch, 1:500) were applied in 1% (w/v) BSA/PBS for 1 h. The neurons were washed three times in PBS, mounted on microscope slides (Aqua Poly/Mount, Polysciences), and observed under a confocal laser scanning microscope (Fluoview 1000, Olympus). The average HA-GABA$_{B2}$ and EGFP fluorescence signal intensities within each of 10 rectangles covering a MAP2-negative neurite were determined using Olympus Fluoview 1.7b software. The mean HA-GABA$_{B2}$/EGFP ratio was calculated as an estimate of the relative axonal HA-GABA$_{B2}$ surface expression. The results from at least 38 MAP2-negative neurites are presented as the means ± S.E. A Student's *t* test was applied to calculate the statistical differences.

## RESULTS

*N- and C-terminal Tandem Affinity Tags on GABA$_{B1}$*—We set out to generate transgenic mice equipped with affinity tags for the purification of GABA$_B$ receptors. To this end, DNA sequences encoding two different TAP tags were independently inserted into BAC citb544e14 (40), which contains a fragment of mouse chromosome 17 including the gene for GABA$_{B1}$, by homologous recombination in *E. coli* (27, 41) (Fig. 1*A*). The classical TAP tag consisting of CBP, the TEV protease recognition site, and protein A was appended to the C terminus of GABA$_{B1}$ (GABA$_{B1}$-CBP-TEV-ProtA). Alternatively, we added a tandem tag consisting of an HA epitope and a SBP to the N terminus of the mature GABA$_{B1a}$ polypeptide (HA-SBP-GABA$_{B1a}$). The purpose of the former construct was to allow purification of GABA$_{B1}$ complexes irrespective of the isoform, whereas the latter should help isolating specifically GABA$_{B1a}$-containing receptors (Fig. 1*B*).

To check for the functional integrity of receptors containing these tags, we employed an aequorin assay. GABA$_{B1a}$ carrying the two different tandem affinity tags at either the N or the C terminus was coexpressed with GABA$_{B2}$ in Chinese hamster ovary/G$\alpha_{16}$/mtAEQ cells (32). The manipulated receptors were indistinguishable from wild-type versions with respect to baclofen-stimulated calcium mobilization (EC$_{50}$(GABA$_{B1a}$/GABA$_{B2}$), 3.3 ± 2.8 $\mu$M; EC$_{50}$(HA-SBP-GABA$_{B1a}$/GABA$_{B2}$), 2.7 ± 2.2 $\mu$M; EC$_{50}$(GABA$_{B1a}$-CBP-TEV-ProtA/GABA$_{B2}$), 3.3 ± 2.5 $\mu$M), indicating that the tags on GABA$_{B1a}$ did not compromise surface expression, ligand binding, or G-protein coupling of the heterodimeric receptor.

*BAC Transgenic Mice Expressing TAP-tagged GABA$_{B1}$*—The modified BACs were injected into oocytes, and the transgenic mouse lines were established (NTAP-GABA$_{B1a}$, GABA$_{B1a/b}$-CTAP). The distribution of the transgenic brain mRNAs detected by *in situ* hybridization at P12 was largely identical to that of the endogenous transcripts in wild-type mice (Fig. 2*A*).

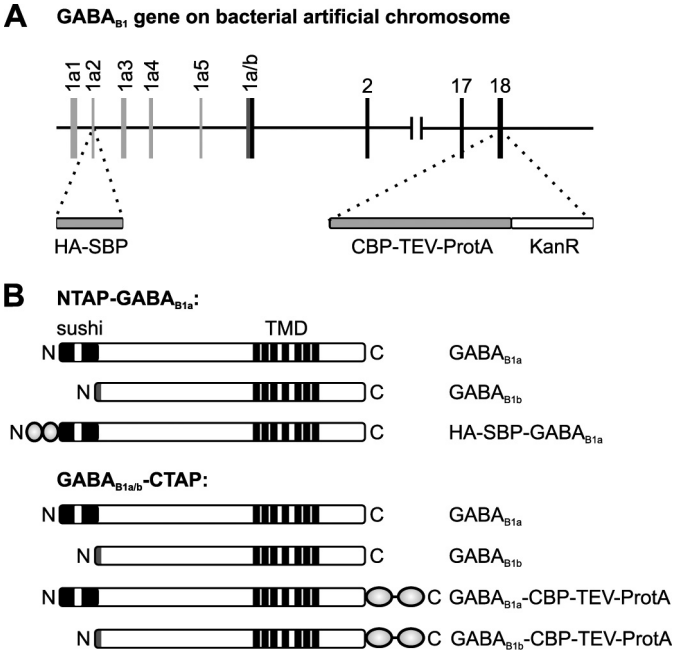


FIGURE 1. **Targeting TAP sequences into the GABA$_{B1}$ gene on BAC citb544e14.** *A*, sequences coding for the HA-SBP tag were introduced into the GABA$_{B1a}$-specific exon 1a2 (6), 3′ to the signal sequence, whereas sequences coding for the CBP-TEV-ProtA tag and a kanamycin resistance gene were inserted into exon 18 (6), 5′ to the stop codon. GABA$_{B1a}$-specific exons are shown in *light gray*, and the GABA$_{B1b}$-specific region of exon 1a/b is in *dark gray*. *B*, scheme of tagged and untagged GABA$_{B1}$ isoforms in the BAC transgenic mice. *TMD*, transmembrane domain; *sushi*, sushi repeat.

However, in GABA$_{B1a/b}$-CTAP mice the transgenic expression appeared slightly more pronounced in cortex and thalamus. Importantly, the BAC-derived messages recapitulated the cell type-specific expression of GABA$_{B1}$ isoforms in the cerebellum known from wild-type mice (42, 43). Furthermore, expression of the TAP-tagged GABA$_{B1}$ proteins was readily detectable on the Western blots of brain membranes from the transgenic mice (Fig. 2*B*; see also Fig. 4*A*).

To confirm that the genetic manipulation did not interfere with physiological GABA$_B$ receptor functions, we assessed the baclofen effects in acute hippocampal slices of NTAP-GABA$_{B1a}$, GABA$_{B1a/b}$-CTAP, and wild-type mice (Fig. 3). Baclofen via activation of presynaptic GABA$_B$ receptors strongly reduced excitatory and inhibitory postsynaptic currents (EPSCs and IPSCs) recorded in CA1 pyramidal cells in all genotypes to similar extents (Fig. 3, *A* and *B*). Comparable increases in holding currents by baclofen in all three genotypes indicated normal postsynaptic GABA$_B$ receptor function (Fig. 3*C*).

*Tandem Affinity Purification of GABA$_{B1}$*—Membrane proteins were solubilized from the brains of transgenic and wild-type mice and subjected to the respective TAP protocol. Western blot analysis of the final fractions (Fig. 4) revealed transgene-specific isolation not only of the tagged proteins, but also of GABA$_{B2}$, indicating that the integrity of the receptors was conserved throughout the purification. Two prominent synaptic proteins not implicated with GABA$_B$ receptors, CASK and PSD-95, were not detectable in the final fractions.

Silver staining of final TAP fractions separated by SDS-PAGE revealed complex patterns but allowed identification of

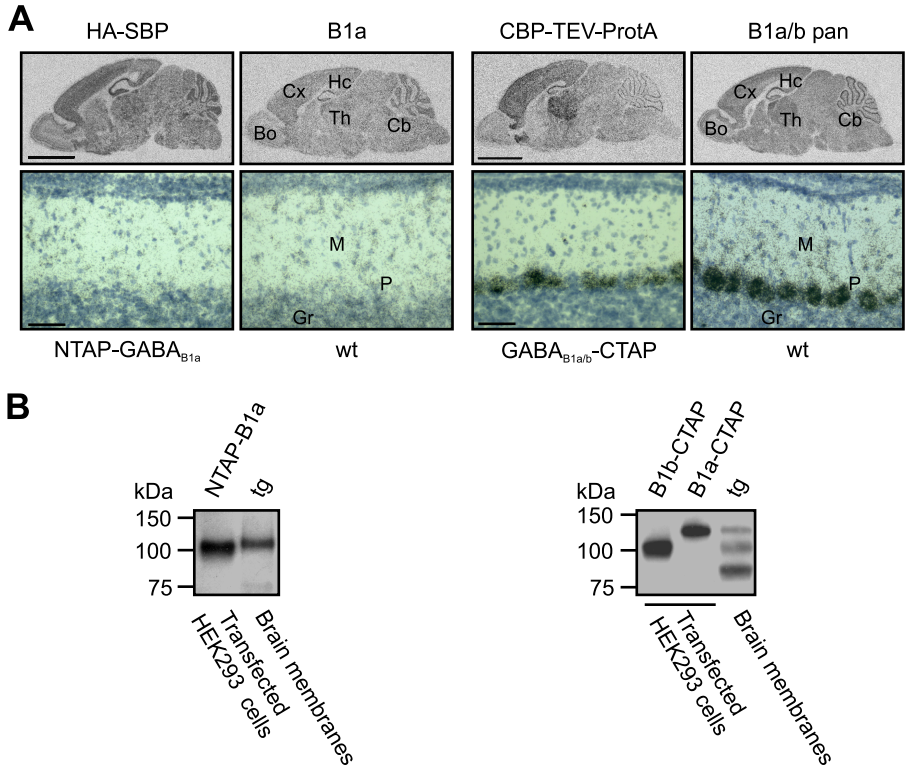


FIGURE 2. **Expression of the transgenes in mouse brain.** *A*, autoradiographic images (*upper panels*) and photomicrographs of the cerebellum (*lower panels*) depicting *in situ* hybridization of radioactively labeled cRNA probes detecting either the transgenic (*HA-SBP*, *ProtA-TEV-CBP*) or the wild-type (*B1a*, *B1a/b pan*) mRNAs at P12. *Hc*, hippocampus; *Cx*, cortex; *Th*, thalamus; *Cb*, cerebellum; *Bo*, bulbus olfactorius; *Gr*, granule cell layer; *M*, molecular layer; *P*, Purkinje cell layer. *Scale bars*, 3 mm in the *upper panels*; 50 $\mu$m in the *lower panels*. *B*, immunoblots detecting the tagged proteins in NTAP-GABA$_{B1a}$ (*left panel*, anti-HA) and GABA$_{B1a/b}$-CTAP (*right panel*, anti-GABA$_{B1}$ pan sc-14006) transgenic mice. The anti-GABA$_{B1}$ blot also reveals GABA$_{B1b}$ (*bottom band* in the *right lane*), whereas GABA$_{B1a}$ comigrates with GABA$_{B1b}$-CBP-TEV-ProtA. *wt*, wild-type; *tg*, transgenic; *NTAP-B1a*, HA-SBP-GABA$_{B1a}$; *B1b-CTAP*, GABA$_{B1b}$-CBP-TEV-ProtA; *B1a-CTAP*, GABA$_{B1a}$-CBP-TEV-ProtA.

bands obviously enriched in the transgenic samples by visual inspection (Fig. 5). These bands and their wild-type counterparts were isolated and subjected to trypsin digestion followed by liquid chromatography-tandem mass spectrometry. The peptide analysis revealed, besides GABA$_B$ receptor subunits, glucose-regulated protein 78 (GRP78/BiP) (44) in samples from NTAP-GABA$_{B1a}$ and potassium channel tetramerization domain-containing protein 12 (KCTD12/pfetin) (45) in samples from GABA$_{B1a/b}$-CTAP mice (Table 1).

Western blots of the final TAP fractions confirmed the mass spectrometric identification of the two candidate GABA$_B$ receptor interactors (Fig. 6, *A* and *B*). Moreover, anti-GABA$_{B1}$ immunoprecipitates from wild-type mice contained both GRP78 and KCTD12, corroborating them as constituents of native GABA$_{B1}$ receptor complexes (Fig. 6*C*).

*The T1 Domain of KCTD12 Interacts with GABA$_B$ Receptors via the C Terminus of GABA$_{B2}$*—The interaction between KCTD12 and the GABA$_B$ receptor was further assessed in transfected HEK293 cells (Fig. 7). KCTD12 bound to GABA$_{B2}$ and not to GABA$_{B1}$ and allowed formation of a ternary complex consisting of GABA$_{B1}$, GABA$_{B2}$, and KCTD12. We mapped the KCTD12 interaction site in GABA$_{B2}$ to a region of the C terminus distal to the membrane (amino acids 817–920). GABA$_{B2}$ binding was mediated by an N-terminal fragment of KCTD12 encompassing a voltage-gated potassium channel tetramerization (T1) domain (45). Thus, KCTD12 appears to interact with functional GABA$_B$ receptors by T1 domain binding to the C-terminal region of GABA$_{B2}$.

*Influence of KCTD12 on the Neuronal Distribution of GABA$_B$ Receptors*—Transfection of KCTD12 constructs into primary neurons from rat hippocampus altered the distribution of coexpressed HA-GABA$_{B2}$ (Fig. 8). KCTD12 increased the amount of HA-GABA$_{B2}$ at the surface of neurites. This effect was largely confined to regions that were negative for the dendritic marker MAP2. These data suggest that KCTD12 supports GABA$_{B2}$ surface expression primarily in axonal domains. Thus, KCTD12 may have an impact on the axonal transport or surface stability of GABA$_B$ receptors.

## DISCUSSION

Here we used tandem affinity purification from mouse brain to identify proteins associated with the GABA$_B$ receptor subunit GABA$_{B1}$. As expected from a BAC approach, mRNAs for the tagged receptor subunits were distributed similarly to their endogenous counterparts, and the proteins were not strongly overexpressed by the genetic manipulation. In addition, the physiological pre- and postsynaptic effects of GABA$_B$ receptors were preserved. Thus, GABA$_{B1}$ complexes isolated from these mice have a good chance to mimic the *in vivo* situation. The mice should therefore offer a convenient way to unravel native GABA$_{B1}$ complexes. However, visual inspection of silver-stained gels loaded with purified fractions from transgenic and wild-type mice yielded a small number of complex-specific protein bands. This limitation is attributed to unspecific binding to the affinity matrices under the described conditions, which probably reflects the tagged target protein GABA$_{B1}$ being only a minute constituent within the solubilized brain membranes used as source. The highest expression of GABA$_{B1a}$ occurs during the first postnatal days (3). We therefore tried purification from newborn NTAP-GABA$_{B1a}$ mice but observed a pattern of silver-stained protein bands virtually identical to the one from P10-P16 mice.

The HA-SBP tag combination introduced here may offer advantages as compared with the established CBP-TEV-ProtA tag. The HA-SBP tag is rather small (56 amino acids; ~6 kDa) and might therefore show less interference with the trafficking and function of tagged target molecules. Moreover, substitution of the CBP tag may be preferred for purification from tissues with significant expression of calmodulin. However, we

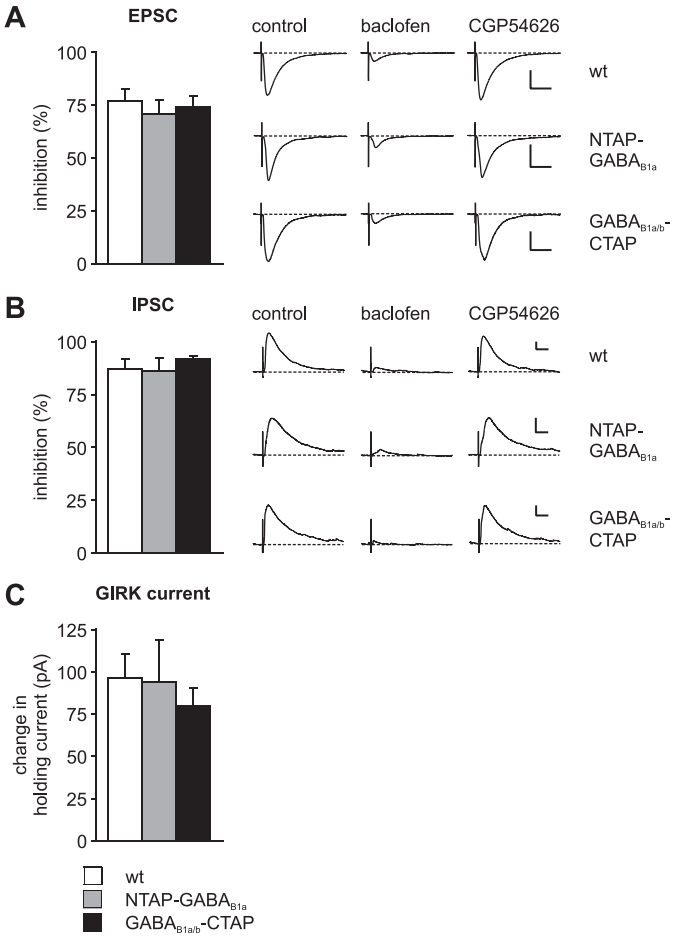


FIGURE 3. **GABA$_B$ receptor activation in the hippocampus of wild-type and BAC transgenic mice.** *A*, peak amplitudes of EPSCs recorded in CA1 neurons at −80 mV were similarly ($p > 0.05$) reduced in the presence of baclofen (50 $\mu$M) in wild-type ($n = 8$), NTAP-GABA$_{B1a}$ ($n = 5$), and GABA$_{B1a/b}$-CTAP ($n = 5$) transgenic mice, as summarized in the *bars* and illustrated by representative current traces. *Scale bars*, 100 pA, 20 ms. *B*, peak amplitudes of IPSCs recorded at 0 mV were similarly ($p > 0.05$) reduced by baclofen (50 $\mu$M) in wild-type ($n = 6$), NTAP-GABA$_{B1a}$ ($n = 6$), and GABA$_{B1a/b}$-CTAP ($n = 4$) transgenic mice. *Scale bars* for representative current traces, 50 pA, 20 ms. CGP54626 (5 $\mu$M) reversed the baclofen-mediated effects on EPSCs and IPSCs. All of the current traces are the averages of six consecutive traces. *C*, summary of changes in holding current recorded in the presence of tetrodotoxin (1 $\mu$M) at −50 mV following baclofen perfusion, reflecting activation of G-protein-regulated inwardly rectifying potassium channel currents in wild-type ($n = 7$), NTAP-GABA$_{B1a}$ ($n = 3$), and GABA$_{B1a/b}$-CTAP ($n = 4$) transgenic mice. *wt*, wild-type.

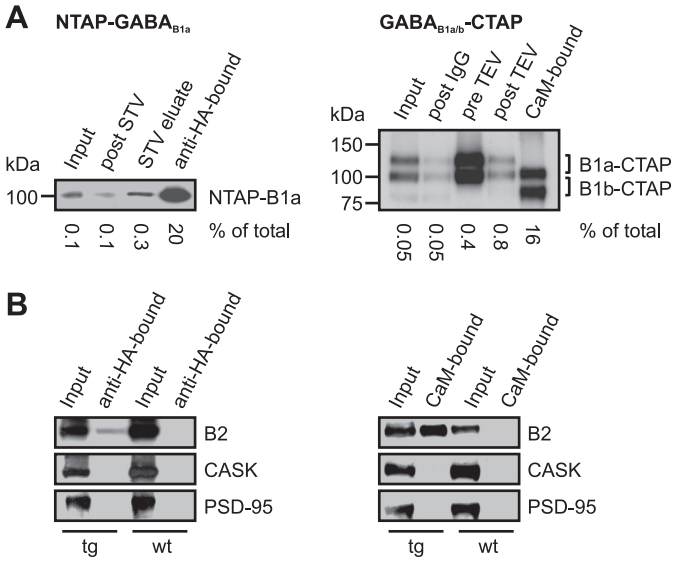


FIGURE 4. **Tandem affinity purification of GABA$_B$ receptors from transgenic mouse brains.** *A, left panel*, immunoblot of NTAP-GABA$_{B1a}$ purification steps stained with an anti-HA antibody; *post STV*, extract after incubation with the streptavidin (*STV*) matrix; *STV eluate*, protein eluted with biotin from the STV matrix. *A, right panel*, immunoblot of GABA$_{B1a/b}$-CTAP purification steps stained with an anti-GABA$_{B1}$ pan antibody (AB1531). *post IgG*, extract after incubation with the IgG matrix; *pre TEV*, IgG-bound protein prior to TEV protease cleavage; *post TEV*, eluate of the IgG matrix after incubation with TEV protease. Anti-GABA$_{B1}$ AB1531 strongly reacted with protein A revealing primarily the TAP-tagged variants (compare with Fig. 2*B*). *B*, immunoblots of input and final TAP fractions prepared from the transgenic lines (*tg*) and wild-type (*wt*) control animals. *B2*, GABA$_{B2}$; *PSD-95*, postsynaptic density protein 95.

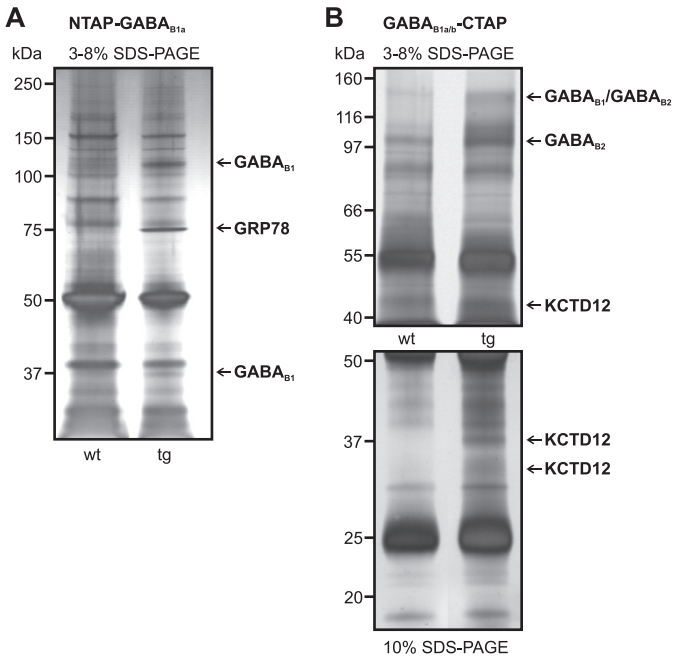


FIGURE 5. **Mass spectrometric identification of GRP78/BiP and KCTD12 as potential GABA$_{B1}$-binding proteins.** Shown are silver-stained SDS-PAGE of the final TAP fractions prepared from NTAP-GABA$_{B1a}$ (*A*) or GABA$_{B1a/b}$-CTAP (*B*) mice and wild-type controls. A 50% excess of wild-type material was loaded to facilitate the identification of protein bands specifically enriched in the transgenic fractions. These bands, which are marked by *arrows*, and the corresponding regions from the wild-type control lanes were analyzed using mass spectrometry (Table 1).

noted an unexpected loss of GABA$_{B2}$ specifically during purifications from NTAP-GABA$_{B1a}$ mice (Fig. 4*B*). It is possible that the HA tag is better accessible in unassembled HA-SBP-GABA$_{B1a}$ than in the heterodimer. The fact that we did not find KCTD12 in the NTAP-GABA$_{B1a}$ samples may result from the loss of GABA$_{B2}$.

Our data show that the chaperone protein GRP78 bound to GABA$_{B1}$ *in vivo*. Purified samples from NTAP-GABA$_{B1a}$ mice routinely showed a conspicuously strong band migrating slightly more slowly than a 75-kDa marker protein, which was identified as GRP78 by mass spectrometry. GRP78 is a luminal endoplasmic reticulum protein mainly involved with chaperone functions and the unfolded protein response (44, 46, 47). However, a control Western blot suggested that the transgenic receptor subunits did not lead to an obvious induction of GRP78, which would have been expected in the case of an endoplasmic reticulum stress response (Fig. 6*A*). In addition, we detected GRP78 not only in purified fractions from both trans-

**TABLE 1**

**Proteins identified from liquid chromatography-tandem mass spectrometry analysis of TAP fractions**

Protein bands enriched in NTAP-GABA$_{B1a}$ or GABA$_{B1a/b}$-CTAP fractions (Fig. 4) were analyzed by liquid chromatography-tandem mass spectrometry. All of the unambiguously identified peptide sequences from the corresponding proteins are listed along with the score of the identification reported from the Mascot search engine and the deviation of the experimentally determined mass from the theoretical in parts per million. The asterisk indicates peptides also identified in wild-type control samples.

| | | NTAP-GABA$_{B1a}$ | | GABA$_{B1a/b}$-CTAP | |
|---|---|---|---|---|---|
| Protein | Peptide Sequence | Mascot Score | Mass Error (ppm) | Mascot Score | Mass Error (ppm) |
| GABA$_{B1}$ | AINFLPVDYEIEYVCR | 27 | 0.38 | 69 | 0.39 |
| | CDPDFHLVGSSR | | | 48 | 0.19 |
| | DILPDYELK* | | | 32 | 0.22 |
| | EAGIEITFR | | | 33 | 0.50 |
| | ELEKIIAEKEER | | | 50 | 0.64 |
| | GEREVVGPK | 30 | 0.45 | 26 | 0.63 |
| | GEWQSEAQDTMK | | | 48 | 0.06 |
| | GLTRDQVK | 35 | 0.51 | | |
| | IGYYDSTK | | | 34 | 1.09 |
| | IIAEKEER | | | 47 | 0.19 |
| | IIVGLFYETEAR* | 59 | 0.71 | 74 | 0.14 |
| | KVFCEVYK | | | 37 | 2.58 |
| | KVFCEVYKER | | | 46 | 0.04 |
| | LLEKENR | | | 35 | 1.28 |
| | QRFPTFFR | 31 | 0.77 | 38 | 0.45 |
| | QSFFSDPAVPVK | 52 | 0.86 | 54 | 0.93 |
| | RDILPDYELK | | | 31 | 7.46 |
| | SYLTLENGK | 47 | 0.42 | 57 | 0.76 |
| | SYLTLENGKVFLTGGDLPALDGAR | | | 26 | 1.83 |
| | THPSATLHNPTR | 26 | 0.11 | 34 | 0.50 |
| | TIETFAK | | | 25 | 1.21 |
| | VFCEVYKER | | | 35 | 1.50 |
| | VFLTGGDLPALDGAR | 47 | 1.20 | 76 | 1.24 |
| | VKEAGIEITFR | | | 72 | 2.21 |
| | YLYELLYNDPIK | | | 61 | 1.29 |
| GABA$_{B2}$ | AMETLHASSR | | | 71 | 1.16 |
| | FQFTQNQK | | | 25 | 1.86 |
| | FTQFQDSR | | | 31 | 0.79 |
| | IILGQFDQNMAAK | | | 61 | 1.23 |
| | KYPYFFR | | | 25 | 0.24 |
| | LEGLQSENHR | | | 56 | 1.37 |
| | LYDTECDNAK | | | 43 | 1.42 |
| | RFQFTQNQK | | | 28 | 0.96 |
| | RVGTLTQDVQR | | | 39 | 0.44 |
| | TFETLCTVR | | | 44 | 1.04 |
| | TIILEQLR | | | 48 | 0.15 |
| | TNPDAATQNR | | | 42 | 0.21 |
| | TPQQYER | | | 54 | 0.37 |
| | TSTSVTSVNQASTSR | | | 67 | 1.25 |
| | TVPSDNAVNPAILK | | | 69 | 0.18 |
| | VGTLTQDVQR* | | | 73 | 1.29 |
| | YSMEPDPAGR | | | 31 | 0.46 |
| GPR78 | DAGTIAGLNVMR | 64 | 0.41 | | |
| | ELEEIVQPIISK | 40 | 0.41 | | |
| | IINEPTAAAIAYGLDKR | 32 | 0.16 | | |
| | ITITNDQNR | 34 | 0.02 | | |
| | ITPSYVAFTPEGER | 27 | 1.43 | | |
| | LYGSGGPPPTGEEDTSEKDEL | 51 | 0.09 | | |
| | MKETAEAYLGK | 25 | 0.37 | | |
| | MKETAEAYLGKK | 33 | 0.03 | | |
| | NGRVEIIANDQGNR | 38 | 0.60 | | |
| | NQLTSNPENTVFDAK | 56 | 0.62 | | |
| | QATKDAGTIAGLNVMR | 31 | 0.80 | | |
| | SQIFSTASDNQPTVTIK | 58 | 0.42 | | |
| | TFAPEEISAMVLTK | 40 | 0.16 | | |
| | TKPYIQVDIGGGQTK | 52 | 0.35 | | |
| | TWNDPSVQQDIK | 68 | 0.77 | | |
| | VEIIANDQGNR | 54 | 0.84 | | |
| | VLEDSDLK | 35 | 0.92 | | |
| | VMEHFIK | 34 | 0.06 | | |
| | VTHAVVTVPAYFNDAQR | 33 | 0.07 | | |
| | VYEGERPLTK | 32 | 0.72 | | |
| KCTD12 | ALADSTR | | | 43 | 2.87 |
| | CTVVSVPDSLLWR | | | 36 | 1.70 |
| | DAQADAKFR | | | 57 | 0.85 |
| | DLQLVLPDYFPER* | | | 52 | 0.44 |
| | EAEYFELPELVR* | | | 42 | 3.01 |
| | EAEYFELPELVRR | | | 26 | 0.32 |
| | EVFGDTLNESR | | | 48 | 2.06 |
| | EVFGDTLNESRD | | | 42 | 0.99 |
| | FFLDRDGFLFR | | | 32 | 0.58 |
| | FNFLEQAFDK | | | 51 | 0.77 |
| | GRFFLDR | | | 37 | 0.45 |
| | GSYTIGR* | | | 35 | 2.01 |
| | GSYTIGRDAQADAK | | | 35 | 0.88 |
| | LQREAEYFELPELVR | | | 39 | 0.71 |
| | MFTQQQPQELAR* | | | 77 | 0.91 |
| | RSGYITIGYR | | | 49 | 1.40 |
| | SGYITIGYR* | | | 42 | 1.14 |
| | SPSGGAAGPLLTPSQSLDGSR* | | | 69 | 0.28 |
| | SPSGGAAGPLLTPSQSLDGSRR* | | | 36 | 0.00 |
| | TSLAKEVFGDTLNESR | | | 54 | 3.08 |
| | YILDYLR* | | | 43 | 1.62 |

genic mouse lines but also in GABA$_{B1}$ complexes immunoprecipitated from wild-type mice. GRP78 binding may mediate the maturation of the GABA$_B$ receptor, possibly by supporting the proper folding of the GABA$_{B1}$ subunit and avoiding its aggregation until the heterodimer is formed. The particularly large amount of GRP78 found in the final fractions of the NTAP-GABA$_{B1a}$ mice may reflect that our purification scheme favored isolation of the unassembled subunit (see above). The detection of a luminal endoplasmic reticulum protein as a binding partner shows that the strategy used here is not limited to the isolation of cytoplasmic components and may therefore ultimately also allow identification of extracellular interactions of GABA$_B$ receptors.

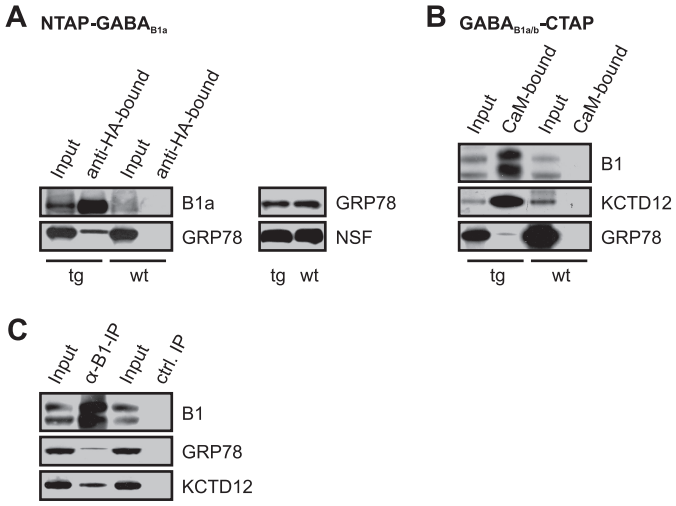


FIGURE 6. **GRP78 and KCTD12 are components of mouse brain GABA$_{B1}$ complexes.** *A* and *B*, immunoblots of input and final TAP fractions prepared from transgenic (*tg*) and wild-type (*wt*) animals. *B1a*, GABA$_{B1a}$; *B1*, GABA$_{B1}$. *A*, *right panel*, immunoblot with GRP78 antibody showing that extracts of NTAP-GABA$_{B1a}$ and wild-type mouse brains contain comparable amounts of GRP78; as a loading control the blot was incubated with an antibody to *N*-ethylmaleimide-sensitive factor (*NSF*). *C*, immunoblots of GRP78 and KCTD12 coimmunoprecipitated (*IP*) with GABA$_{B1}$ from wild-type mouse brains. *Input*: 0.1% in *A*,*B*; 0.5% in *C*. Control (*ctrl*).

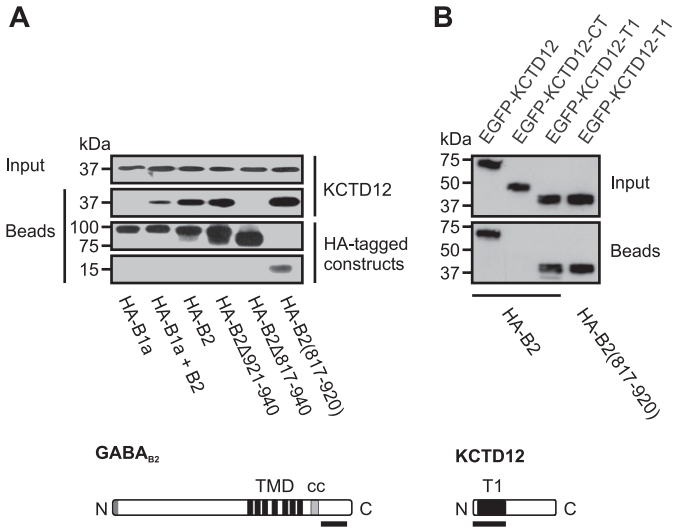


FIGURE 7. **The C terminus of GABA$_{B2}$ engages the T1 domain of KCTD12.** Shown are analyses of anti-HA affinity purifications from HEK293 cells coexpressing HA-tagged receptor constructs with either KCTD12 (*A*) or EGFP-tagged KCTD12 mutants (*B*). Immunoblots with anti-KCTD12 (*A*) or anti-GFP (*B*) antibody reveal the KCTD12 interaction; anti-HA detection (*A*) confirms the integrity of the HA fusion proteins. *Input*, 0.125%. *Bars* beneath the protein schemes (*lower panels*) illustrate the interacting regions in GABA$_{B2}$ (*A*) and KCTD12 (*B*). *cc*, coiled-coil domain.

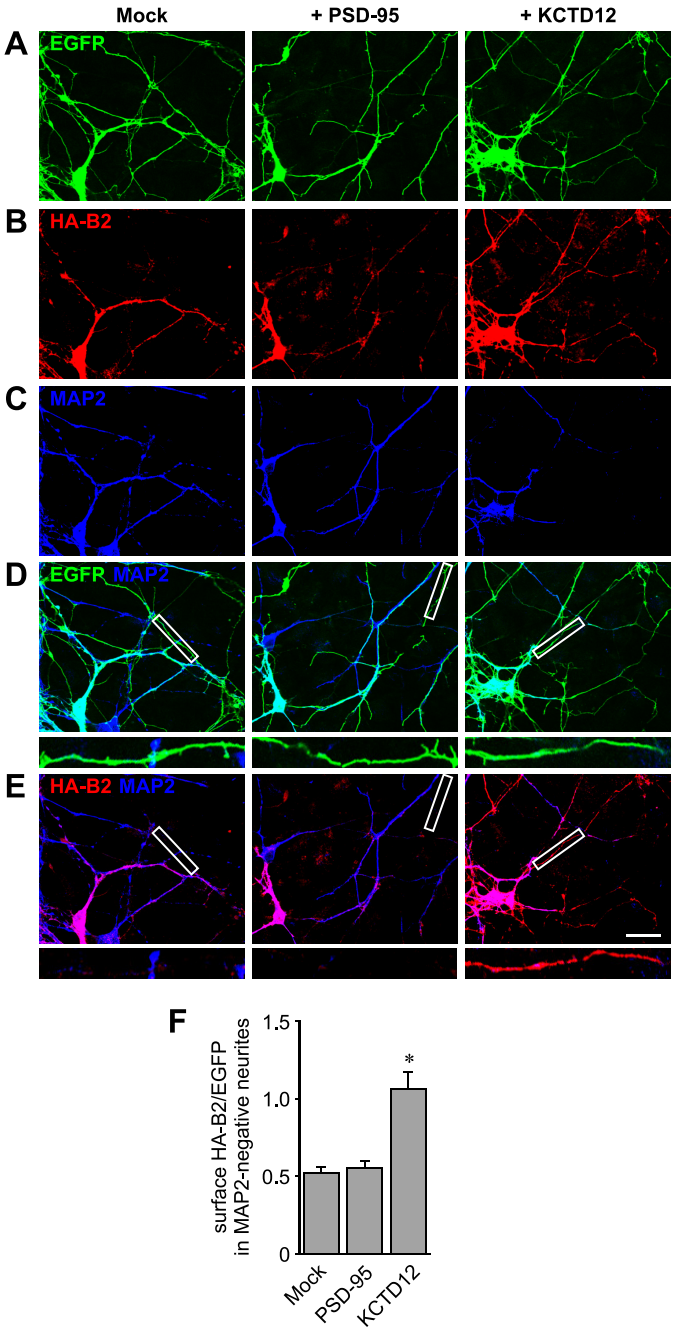


FIGURE 8. **Increased axonal GABA$_{B2}$ expression upon coexpression of KCTD12 in transfected hippocampal neurons.** Primary rat hippocampal neurons were transfected with expression vectors for EGFP, HA-GABA$_{B2}$, and either PSD-95 (+ *PSD-95*), KCTD12 (+ *KCTD12*), or no additional protein (empty vector, *Mock*). The neurons were stained under nonpermeabilizing conditions with an anti-HA antibody and after permeabilization with an antibody directed against the dendritic marker MAP2. Fluorescent signals for EGFP, HA-B2, and MAP2 are shown individually (*A–C*) and as overlays (*D* and *E*). Examples for MAP2-negative neurites of transfected cells are indicated by *white boxes* (enlarged in the *insets*) in *D* and *E*. *Scale bars*, 25 $\mu$m for *large panels*; 7 $\mu$m for *enlarged frames*. *HA-B2*, HA-GABA$_{B2}$. *F*, quantitative analysis of the ratio of the axonal red and green fluorescence intensities. PSD-95, $n$ = 38 axons; Mock, KCTD12, $n$ = 40 axons each. *, $p < 0.0001$.

Our analysis of GABA$_{B1a/b}$-CTAP mice revealed KCTD12 as a novel complex constituent. However, a few peptides for GABA$_{B1}$, GABA$_{B2}$, and KCTD12 were also detected in the samples from wild-type mice, although in small numbers and at lower intensities. Because final fractions of GABA$_{B1a/b}$-CTAP purifications from wild-type mice did not show bands in Western blots with antibodies to GABA$_{B1}$, GABA$_{B2}$, or KCTD12, we ascribe these peptides to contaminations that possibly occurred during isolation of the corresponding bands or the subsequent peptide separation. *KCTD12* has been identified as a gene with predominant fetal expression, most prominently in cochlea and brain (45). KCTD12/pfetin protein was reported to be a prognostic marker for gastrointestinal stromal tumors showing an inverse relation to tumor metastasis (48). The KCTD12 protein contains a T1 domain (45) that belongs to the family of BTB/POZ protein-protein interaction motifs with various cellular functions (49). The T1 domain tetramer of voltage-gated potassium channels subserves $\beta$-subunit association controlling both channel properties and axonal/dendritic targeting (50–55). Interestingly, KCTD12 peptides have also been identified in synaptosomal preparations from mouse brain (56), supporting a role for KCTD12 in synaptic transmission.

With the C-terminal region of GABA$_{B2}$ we report the first binding site for the T1 domain in KCTD12. Importantly, this domain interaction allows association of KCTD12 with the heteromeric, functional GABA$_B$ receptor. Our experiments in transfected dissociated neurons suggest that KCTD12 binding may play a role in transport of the GABA$_B$ receptor to axonal plasma membrane sites reminiscent of the T1 domain in Kv channels (52, 54), implying that T1 domain interactions mediate subcellular targeting of selected neuronal membrane proteins. Given that GABA$_B$ receptors subserve various different functions in dendritic shafts, dendritic spines, and axonal boutons in neurons of the brain, their precise localization is of pivotal importance. In summary, our data introduce the T1 domain protein KCTD12 as an integral part of GABA$_B$ receptors. The TAP-tagged mice may help to unravel the native protein composition of GABA$_{B1}$ complexes in brain and other tissues.

*Acknowledgments—We are grateful to Julia Kuhlmann, Stefanie Wilhelm, Janina Sülflow, and Andrea Zaisser for excellent technical assistance. We thank Irm Hermans-Borgmeyer for oocyte injections, Susanne Fehr for in situ hybridization, Chudamani Rasa Raithore for cultured neurons, and Michaela Schweizer for help with microscopy.*

## REFERENCES

1. Bowery, N. G., Bettler, B., Froestl, W., Gallagher, J. P., Marshall, F., Raiteri, M., Bonner, T. I., and Enna, S. J. (2002) *Pharmacol. Rev.* **54,** 247–264
2. Kulik, A., Vida, I., Luján, R., Haas, C. A., López-Bendito, G., Shigemoto, R., and Frotscher, M. (2003) *J. Neurosci.* **23,** 11026–11035
3. Bettler, B., Kaupmann, K., Mosbacher, J., and Gassmann, M. (2004) *Physiol. Rev.* **84,** 835–867
4. Kaupmann, K., Huggel, K., Heid, J., Flor, P. J., Bischoff, S., Mickel, S. J., McMaster, G., Angst, C., Bittiger, H., Froestl, W., and Bettler, B. (1997) *Nature* **386,** 239–246
5. Peters, H. C., Kämmer, G., Volz, A., Kaupmann, K., Ziegler, A., Bettler, B., Epplen, J. T., Sander, T., and Riess, O. (1998) *Neurogenetics* **2,** 47–54
6. Lamp, K., Humeny, A., Nikolic, Z., Imai, K., Adamski, J., Schiebel, K., and Becker, C. M. (2001) *Cytogenet. Cell Genet.* **92,** 116–121
7. Vigot, R., Barbieri, S., Bräuner-Osborne, H., Turecek, R., Shigemoto, R., Zhang, Y. P., Luján, R., Jacobson, L. H., Biermann, B., Fritschy, J. M., Vacher, C. M., Müller, M., Sansig, G., Guetg, N., Cryan, J. F., Kaupmann, K., Gassmann, M., Oertner, T. G., and Bettler, B. (2006) *Neuron* **50,** 589–601
8. Pérez-Garci, E., Gassmann, M., Bettler, B., and Larkum, M. E. (2006) *Neu-*

*ron* **50,** 603–616
9. Guetg, N., Seddik, R., Vigot, R., Turecek, R., Gassmann, M., Vogt, K. E., Bräuner-Osborne, H., Shigemoto, R., Kretz, O., Frotscher, M., Kulik, A., and Bettler, B. (2009) *J. Neurosci.* **29,** 1414–1423
10. Tiao, J. Y., Bradaia, A., Biermann, B., Kaupmann, K., Metz, M., Haller, C., Rolink, A. G., Pless, E., Barlow, P. N., Gassmann, M., and Bettler, B. (2008) *J. Biol. Chem.* **283,** 31005–31011
11. Blein, S., Ginham, R., Uhrin, D., Smith, B. O., Soares, D. C., Veltel, S., McIlhinney, R. A., White, J. H., and Barlow, P. N. (2004) *J. Biol. Chem.* **279,** 48292–48306
12. Kulik, A., Vida, I., Fukazawa, Y., Guetg, N., Kasugai, Y., Marker, C. L., Rigato, F., Bettler, B., Wickman, K., Frotscher, M., and Shigemoto, R. (2006) *J. Neurosci.* **26,** 4289–4297
13. Tabata, T., Araishi, K., Hashimoto, K., Hashimotodani, Y., van der Putten, H., Bettler, B., and Kano, M. (2004) *Proc. Natl. Acad. Sci. U.S.A.* **101,** 16952–16957
14. Chang, W., Tu, C., Cheng, Z., Rodriguez, L., Chen, T. H., Gassmann, M., Bettler, B., Margeta, M., Jan, L. Y., and Shoback, D. (2007) *J. Biol. Chem.* **282,** 25030–25040
15. Bettler, B., and Tiao, J. Y. (2006) *Pharmacol. Ther.* **110,** 533–543
16. Kornau, H. C. (2006) *Cell Tissue Res.* **326,** 517–533
17. Rigaut, G., Shevchenko, A., Rutz, B., Wilm, M., Mann, M., and Séraphin, B. (1999) *Nat. Biotechnol.* **17,** 1030–1032
18. Gavin, A. C., Bösche, M., Krause, R., Grandi, P., Marzioch, M., Bauer, A., Schultz, J., Rick, J. M., Michon, A. M., Cruciat, C. M., Remor, M., Höfert, C., Schelder, M., Brajenovic, M., Ruffner, H., Merino, A., Klein, K., Hudak, M., Dickson, D., Rudi, T., Gnau, V., Bauch, A., Bastuck, S., Huhse, B., Leutwein, C., Heurtier, M. A., Copley, R. R., Edelmann, A., Querfurth, E., Rybin, V., Drewes, G., Raida, M., Bouwmeester, T., Bork, P., Seraphin, B., Kuster, B., Neubauer, G., and Superti-Furga, G. (2002) *Nature* **415,** 141–147
19. Häcker, H., Redecke, V., Blagoev, B., Kratchmarova, I., Hsu, L. C., Wang, G. G., Kamps, M. P., Raz, E., Wagner, H., Häcker, G., Mann, M., and Karin, M. (2006) *Nature* **439,** 204–207
20. Bürckstümmer, T., Bennett, K. L., Preradovic, A., Schütze, G., Hantschel, O., Superti-Furga, G., and Bauch, A. (2006) *Nat. Methods* **3,** 1013–1019
21. Gregan, J., Riedel, C. G., Petronczki, M., Cipak, L., Rumpf, C., Poser, I., Buchholz, F., Mechtler, K., and Nasmyth, K. (2007) *Nat. Protoc.* **2,** 1145–1151
22. Angrand, P. O., Segura, I., Völkel, P., Ghidelli, S., Terry, R., Brajenovic, M., Vintersten, K., Klein, R., Superti-Furga, G., Drewes, G., Kuster, B., Bouwmeester, T., and Acker-Palmer, A. (2006) *Mol. Cell. Proteomics* **5,** 2211–2227
23. Daulat, A. M., Maurice, P., Froment, C., Guillaume, J. L., Broussard, C., Monsarrat, B., Delagrange, P., and Jockers, R. (2007) *Mol. Cell. Proteomics* **6,** 835–844
24. Schall, T. J., Lewis, M., Koller, K. J., Lee, A., Rice, G. C., Wong, G. H., Gatanaga, T., Granger, G. A., Lentz, R., Raab, H., Kohr, W. J., and Goeddel, D. V. (1990) *Cell* **61,** 361–370
25. Keefe, A. D., Wilson, D. S., Seelig, B., and Szostak, J. W. (2001) *Protein Expression Purif.* **23,** 440–446
26. Grünewald, S., Schupp, B. J., Ikeda, S. R., Kuner, R., Steigerwald, F., Kornau, H. C., and Köhr, G. (2002) *Mol. Pharmacol.* **61,** 1070–1080
27. Zhang, Y., Buchholz, F., Muyrers, J. P., and Stewart, A. F. (1998) *Nat. Genet.* **20,** 123–128
28. Gay, P., Le Coq, D., Steinmetz, M., Ferrari, E., and Hoch, J. A. (1983) *J. Bacteriol.* **153,** 1424–1431
29. Dean, D. (1981) *Gene* **15,** 99–102
30. Narayanan, K., Williamson, R., Zhang, Y., Stewart, A. F., and Ioannou, P. A. (1999) *Gene Ther.* **6,** 442–447
31. Nagy, A. (2003) *Manipulating the Mouse Embryo: A Laboratory Manual*, 3rd Ed., Cold Spring Harbor Laboratory, Cold Spring Harbor, NY
32. Stables, J., Green, A., Marshall, F., Fraser, N., Knight, E., Sautel, M., Milligan, G., Lee, M., and Rees, S. (1997) *Anal. Biochem.* **252,** 115–126
33. Hartmann, D., Fehr, S., Meyerhof, W., and Richter, D. (1995) *Dev. Neurosci.* **17,** 246–255
34. Shevchenko, A., Wilm, M., Vorm, O., and Mann, M. (1996) *Anal. Chem.* **68,** 850–858
35. Prokhorova, T. A., Rigbolt, K. T., Johansen, P. T., Henningsen, J., Kratchmarova, I., Kassem, M., and Blagoev, B. (2009) *Mol. Cell. Proteomics* **8,** 959–970
36. Rappsilber, J., Ishihama, Y., and Mann, M. (2003) *Anal. Chem.* **75,** 663–670
37. Blagoev, B., Ong, S. E., Kratchmarova, I., and Mann, M. (2004) *Nat. Biotechnol.* **22,** 1139–1145
38. Olsen, J. V., de Godoy, L. M., Li, G., Macek, B., Mortensen, P., Pesch, R., Makarov, A., Lange, O., Horning, S., and Mann, M. (2005) *Mol. Cell. Proteomics* **4,** 2010–2021
39. Perkins, D. N., Pappin, D. J., Creasy, D. M., and Cottrell, J. S. (1999) *Electrophoresis* **20,** 3551–3567
40. Takada, T., Kumánovics, A., Amadou, C., Yoshino, M., Jones, E. P., Athanasiou, M., Evans, G. A., and Fischer Lindahl, K. (2003) *Genome Res.* **13,** 589–600
41. Nefedov, M., Williamson, R., and Ioannou, P. A. (2000) *Nucleic Acids Res.* **28,** E79
42. Billinton, A., Upton, N., and Bowery, N. G. (1999) *Br. J. Pharmacol.* **126,** 1387–1392
43. Bischoff, S., Leonhard, S., Reymann, N., Schuler, V., Shigemoto, R., Kaupmann, K., and Bettler, B. (1999) *J. Comp. Neurol.* **412,** 1–16
44. Lee, A. S. (2001) *Trends Biochem. Sci.* **26,** 504–510
45. Resendes, B. L., Kuo, S. F., Robertson, N. G., Giersch, A. B., Honrubia, D., Ohara, O., Adams, J. C., and Morton, C. C. (2004) *J. Assoc. Res. Otolaryngol.* **5,** 185–202
46. Li, J., and Lee, A. S. (2006) *Curr. Mol. Med.* **6,** 45–54
47. Goloubinoff, P., and De Los Rios, P. (2007) *Trends Biochem. Sci.* **32,** 372–380
48. Suehara, Y., Kondo, T., Seki, K., Shibata, T., Fujii, K., Gotoh, M., Hasegawa, T., Shimada, Y., Sasako, M., Shimoda, T., Kurosawa, H., Beppu, Y., Kawai, A., and Hirohashi, S. (2008) *Clin. Cancer Res.* **14,** 1707–1717
49. Stogios, P. J., Downs, G. S., Jauhal, J. J., Nandra, S. K., and Privé, G. G. (2005) *Genome Biol.* **6,** R82
50. Gulbis, J. M., Zhou, M., Mann, S., and MacKinnon, R. (2000) *Science* **289,** 123–127
51. Minor, D. L., Lin, Y. F., Mobley, B. C., Avelar, A., Jan, Y. N., Jan, L. Y., and Berger, J. M. (2000) *Cell* **102,** 657–670
52. Gu, C., Jan, Y. N., and Jan, L. Y. (2003) *Science* **301,** 646–649
53. Long, S. B., Campbell, E. B., and Mackinnon, R. (2005) *Science* **309,** 897–903
54. Rivera, J. F., Chu, P. J., and Arnold, D. B. (2005) *Eur. J. Neurosci.* **22,** 1853–1862
55. Xu, M., Cao, R., Xiao, R., Zhu, M. X., and Gu, C. (2007) *J. Neurosci.* **27,** 14158–14170
56. Munton, R. P., Tweedie-Cullen, R., Livingstone-Zatchej, M., Weinandy, F., Waidelich, M., Longo, D., Gehrig, P., Potthast, F., Rutishauser, D., Gerrits, B., Panse, C., Schlapbach, R., and Mansuy, I. M. (2007) *Mol. Cell. Proteomics* **6,** 283–293